Chapter 7
Special Topics in Cryostat Design

Wolfgang Stautner

Abstract This chapter describes a series of special topics that, while coming from the development of Magnetic Resonance Imaging cryostats, are applicable to many other cryostat designs as well. The topics are: boil off minimization, cryocooler integration, designing with inclined tubes and pressure relief and venting. This chapter contains many figures, tables, equations, design algorithms and references useful to cryostat designers.

7.1 Boil off Minimization for Cryostats Without a Cryocooler

This section gives an example calculation for finding the optimal thermal position and length required for linking a thermal shield to a neck tube that supports the helium vessel for minimizing helium boil off (BOFF) [1]. Figure 7.1 shows a typical neck design and Fig. 7.2 shows the model being examined.

The heat balance equation at node T1 is then written as follows:

$$\text{At node T1:} \quad R_{31} - R_{10} - C_{11} + C_{21} - C_{00} + C_{02} = 0 \tag{7.1}$$

The positional variability is indicated by the double arrow at node T1 and X. Note that T3 refers to the temperature of a liquid nitrogen reservoir, usually 80 K.

Where in Fig. 7.2 and Eq. 7.1:

T1 Node temperature of thermal shield at e.g. 40 K

T2 Contact temperature of LN2 reservoir or similar with helium vessel suspension tube

T3 Temperature of liquid nitrogen vessel or thermal shield with temperature T3 (can be higher or lower than T2 to simulate e.g. contact resistance at T2)

W. Stautner (✉)
GE Global Research, Electromagnetics and Superconductivity Lab,
One Research Circle, Niskayuna, NY 12309, USA
e-mail: stautner@research.ge.com

J.G. Weisend II (ed.), *Cryostat Design*, International Cryogenics Monograph Series,
DOI 10.1007/978-3-319-31150-0_7

Fig. 7.1 Typical neck tube with copper links using ultrasonic soldering for consistent thermal contact resistance quality of the copper/steel interfaces

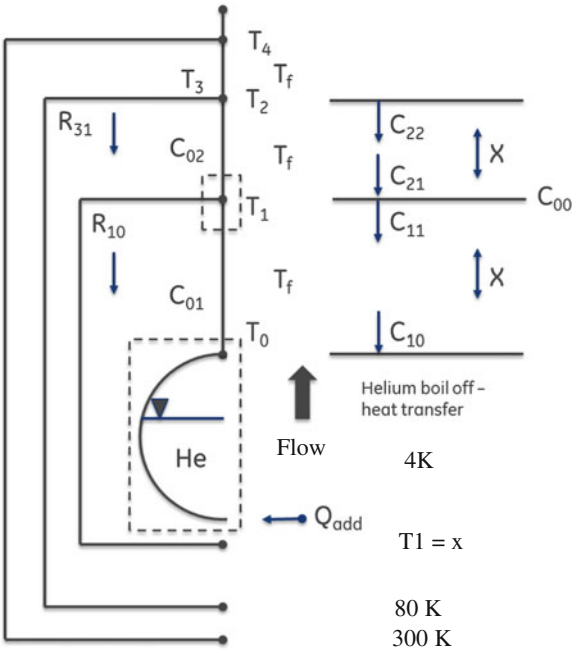

Fig. 7.2 Modeling heat transport and required contact length to achieve minimum BOFF

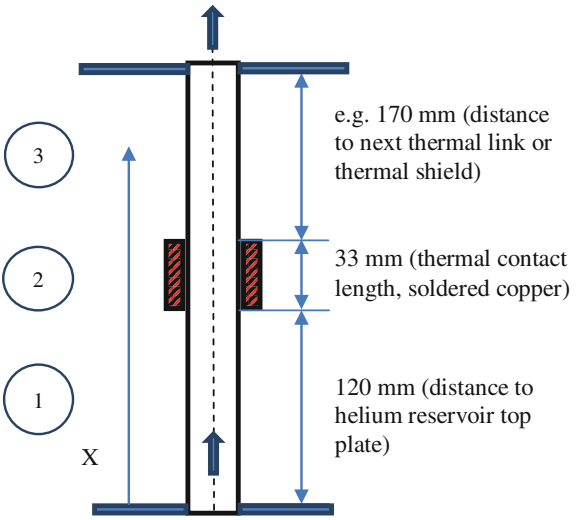

Fig. 7.3 Tube layout as shown in the example

T4 Temperature of vacuum vessel surrounding liquid nitrogen vessel
R_{31} Thermal radiation from 80 K shield to the intermediate shield temperature
R_{10} Thermal radiation from the intermediate shield temperature to helium reservoir
C_{22} Thermal conduction from liquid nitrogen vessel or thermal shield at this location
C_{21} Thermal conduction at tube bottom into node T1
C_{11} Thermal conduction leaving location T1 entering tube connected to helium vessel
C_{10} Thermal conduction at tube bottom connected to helium vessel
C_{00} Conductive heat loade.g. heat sink to external node leaving thermal boundary at node T1
C_{01} Conduction term due to residual gas (vacuum) to helium vessel (can also be used to simulate contact resistance etc.)
C_{02} Conduction term due to residual gas (vacuum) to intermediate thermal shield (can also be used to simulate contact resistance etc.)
Q_{add} Extra heat term to simulate thermal conduction heat load (e.g. suspensions)

Variables:

λ_{Helium} and λ_{Steel} = variable thermal conductivities for helium and steel
cp_{Helium} = constant average value between T0 and T1 or T1 and T2
$R_{31} \neq R_{10}$ = thermal radiation
$Nu_1 \neq Nu_2 \neq Nu_3$ = Nusselt number for each tube section
T3 ≠ T2 = Temperatures can differ
ε tube 1 ≠ ε tube 2 = tube emissivity coefficient can differ

There are different ways of solving the heat balance equations. A particular useful exercise is the finite difference equation (FDE) approach since this allows you to change the tube structure for each node along the tube length. The equations for conduction, convection, radiation and gas flow as written down by Dusinberre [2, 3] and Croft [4]. The software Kryom Version 3.3 also gives you a good initial estimate on the thermal link position and boil off [5] (Table 7.2).

The energy balance equations solved with FDE for each node are conveniently written as:

$$C_{21} - C_{11} + R_{21} - R_{10} = 0; \tag{7.2}$$

$$C_{10} + C_{add} + R_{10} = H_{1v}; \tag{7.3}$$

$$C_{11} - C_{10} = H_{10} \tag{7.4}$$

$$C_{22} - C_{11} = H_{21}. \tag{7.5}$$

(with conduction and thermal radiation terms as shown in Fig. 7.2 and the increase in enthalpy H_{10} and H_{21} of helium gas and with H_{lv} as the product of latent heat and boiling off helium and considering boil off in ullage space).

We now iteratively search for the best TS link position that results in minimum boil off. Furthermore, we obtain information on thermal shield temperature and the profile along the neck tube (see Fig. 7.4). In addition we also get quantitative results on the individual heat flow parameters for the cryogenic design.

Table 7.1 Typical neck tube assembly input parameters as shown in Fig. 7.3

He − TS − LN_2 (K)	4	42 (start value)	80	Temperatures
Nu1 − Nu2 − Nu3 (–)	4	4	4	Nusselt number
dx1 − dx2 − dx3 (mm)	1	1	1	FDE length
Positions (1/2/3)	120	33	170	Tube length
Ra/Ri (mm)	15/14.5			Tube radii
Emissivity coeff ε (–)	0.07/0.065			Thermal radiation
He − TS − LN_2 (m^2)	2.45	1.95	1.76	Cryogenic surfaces

Table 7.2 Results with Table 7.1 parameters

Thermal radiation (R_{31}) (mW)	0.138
Thermal radiation (R_{10}) (mW)	0.0139
Thermal conduction (C_{10}) (mW)	1.02
Thermal conduction (C_{22}) (mW)	127
Thermal conduction (C_{21}) (mW)	18
Thermal conduction (C_{add}) (mW)	1
Optimal TS temperature (K)	44.6
Optimal contact location (mm)	120
Optimal TS/Cu contact length (mm)	33
Minimum boil off per tube (ml/h)	19

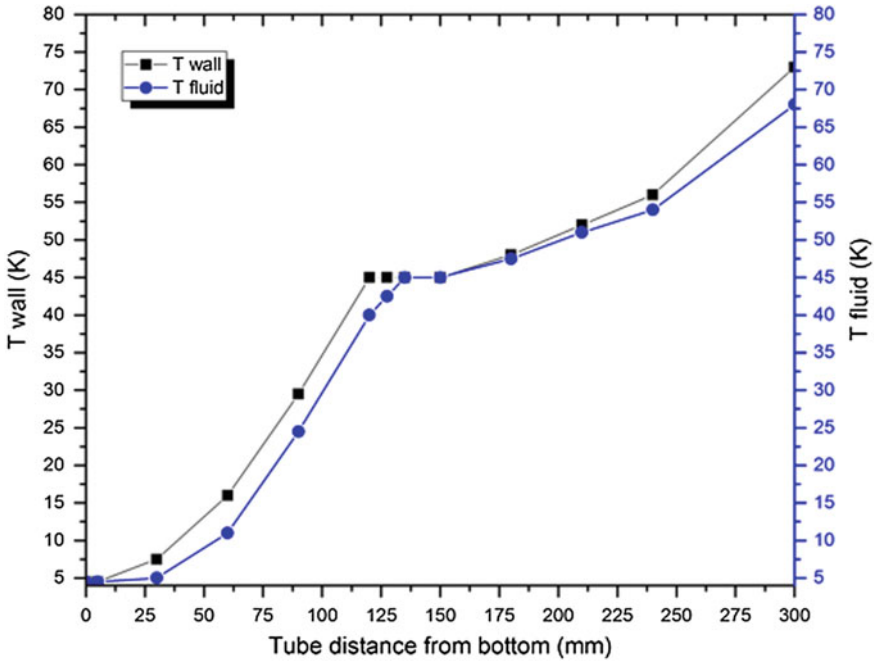

Fig. 7.4 Optimum thermal link position and required contact length for 290 mm SS tube, 25.4 mm

One can modify the FDE nodes to include annular tubes, corrugated tubes, multiple thermal shields or even forced flow.

7.1.1 Discussion

The process of optimizing boil off of a helium vessel can be explained as follows. Once a thermal link from the TS to the neck tube is made, the heat balance around T1 changes correspondingly until equilibrium between all heat sources is obtained and a continuous boil off rate is established.

Figure 7.5 shows how the parameters within this heat balance node T1 change if the TS link position is moved. If the link, for example, is made higher up the neck tube (Figs. 7.2 and 7.3), the amount of heat conducted down from T2 to T1 increases. As a result, the thermal shield temperature increases as well but since the tube length from T1 to T0 increased boil off will be lower. The designer therefore tries to find the minimum as shown in the curves in Fig. 7.5.

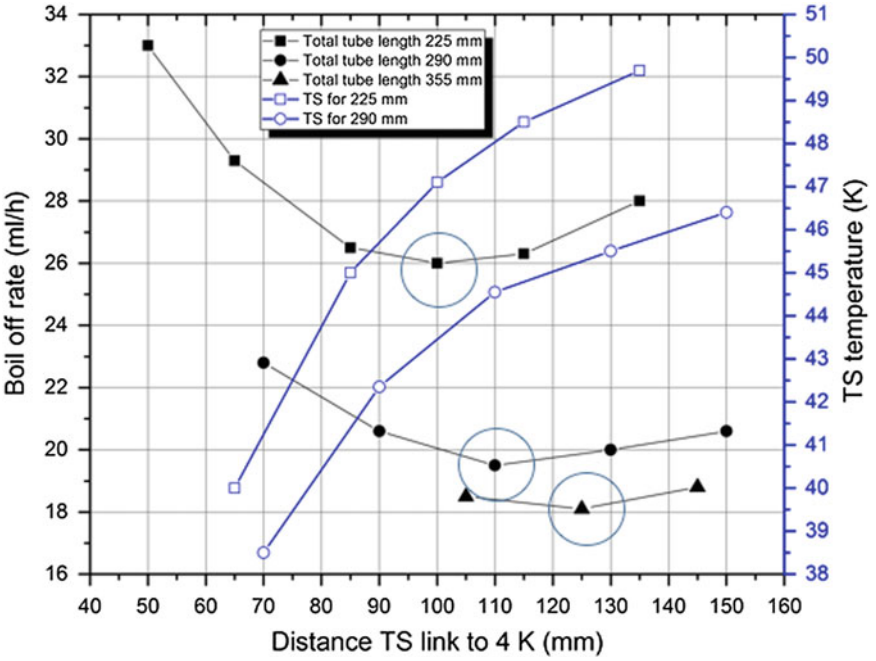

Fig. 7.5 Optimal thermal shield temperature, link position and minimum BOFF

7.1.2 Pitfalls

Minimizing boil off is even more important for multiple tubes in contact with a helium vessel. The problem here is to design the tube arrangement in way that all tubes will be receiving the same mass flow rate. In case of flow restrictions at the neck tube bottom (for example a siphon entry tube or a current lead receptacle) the flow along the tubing will not be evenly distributed. The flow restriction can occur in the tube itself in the form of wire looms or copper baffles. Experiments confirmed the existence of large temperature differences between wall and fluid in this case.

For small boil off flow the Nusselt number is almost always 4 [6] which relates to perfect heat transfer between gas and wall. For imperfect heat transfer and non-optimized neck tubes higher boil off rates will be obtained and the temperature difference between wall and gas can become quite large calling for a longer copper link to “lift” up the gas temperature.

The design for minimum boil-off results in efficient cryogen recondensation and re-liquefaction. In times of high cost of helium; re-liquefaction of helium gas, even for smaller cryogenic systems, is convenient and often advisable.

7.2 Cryocooler Integration

Since their commercial availability in the 1980s, cryocoolers have become excellent and versatile tools for a diverse range of cryogenic applications, from heat sinking a cold mass, to distributed cooling and even for liquefying or dedicated component cooling. At the cryogenic design stage, the cryogenic engineer needs to know in which way the chosen cooler: Gifford-McMahon (GM), Pulse Tube Refrigerator (PTR) or Stirling type can be integrated in a cryogenic structure and in particular how the thermal links to the cryocooler cold stages should be made.

Generally, the cryocooler interface cost is driven up significantly when demanding minimum temperature difference and by associated requirements, e.g. low vibration transmission, or when it is necessary to retract or remove the cooler. Cryogenic designs have to balance this contact quality effort and make a trade-off against what is needed and is feasible for assembly and cooler maintenance. The most common design solutions for dedicated applications are therefore listed below and illustrated in the following examples.

7.2.1 Cryocooler Integration—Options Overview

Cryocooler attachments for thermal mass cooling

- Fixed — bolt on, braided, internal cryocooler parts removable
- Sleeved — sleeve bolt-on or braided, cryocooler removable from sleeve/serviceable
- Un-sleeved — cryocooler exposed to cryogenic atmosphere, e.g. GM/PTR cooler in helium gas
- Retractable — temporarily engage/disengage from cold mass, e.g. after initial cool-down, sleeved

Cryocooler attachments for specialty applications, distributed cooling and component cooling

- Liquefying coolers (fins machined onto cooler cold stage/recondensing fins in standalone cup)
- Heat-sinked heat pipes
- Heat-sinked current leads
- With heat exchanger (HX) and fan-assisted coolant flow
- Remote cold finger

7.2.2 Cryocooler Integration Examples

A good example for directly embedding a pulse tube cooler (PTR) in the coil former of the superconducting magnet cold mass itself is the head imaging prototype system built by GE Global Research back in 1995 (see Fig. 7.6). Technically, this is a bold approach since the cooler cannot be removed, but due to the absence of a moving piston no vibrations are transmitted to the superconducting magnet structure. Furthermore, this cooler does not have to be serviced but can be purged of contaminants when warmed up to room temperature, if necessary.

Direct cryocooler cold mass bolt-on is also an interesting option for a number of small-scale MRI magnet systems using medium or high-temperature superconductors (HTS), see also (1) in Fig. 7.14.

Another early, interventional Helium-free LTS MRI magnet system [8] (see Fig. 7.7) built by GE also used fixed installed cryocoolers. Other than PTRs, GM type coolers tend to transmit their piston vibrations to any connected structure. To mitigate this effect flexible braids are introduced between the interfaces to avoid any ghosting appearing in MRI images.

Both coolers in Fig. 7.7 are sleeved to allow the removal of the cooler from the cold plate during service. The cold plate or heat bus extends from the left to the right of both Helmholtz style superconducting Nb_3Sn coils, operating at 10–11 K.

Note that un-sleeved GM coolers can also be serviced if required, by carefully removing the internal piston assembly from the cooler shell tubing. In this case a warm swap to room temperature may be required which requires a cold mass warm up, unless the cooler envelope can be heated to a high enough temperature to allow servicing or refurbishment.

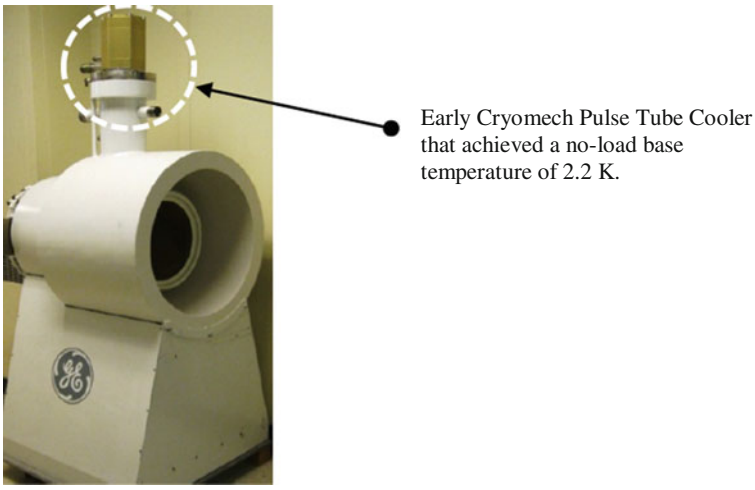

Fig. 7.6 GE 0.5 T conduction-cooled head imaging system [7]

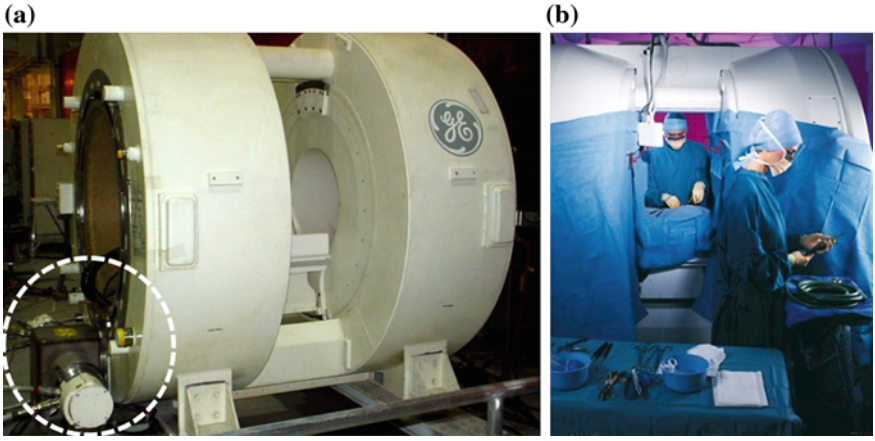

Fig. 7.7 **a** Cryocoolers (2) (*dotted line*) in cold box and in contact with SC coils via heat bus. **b** Surgeons in the operating theater

7.2.3 *Schematics and Options of Cryocooler Integration—Overview*

Figure 7.8 shows the most simple and straightforward way of achieving a good thermal contact across the interfaces. The cryocooler comes with bolt holes on the stages for bolting on to a thermal shield or a cold mass. Since the thermal shrinkage at the stages needs to be considered, bolts with Belleville washers are advisable in case of frequent warm up/cooldown.

A typical cryocooler bolt-on configuration for vibration isolation is shown schematically in Fig. 7.9.

For a description of other common flexible conductive links: braids, foils etc., see also [9].

Figure 7.10 shows the race track test coil cooling [10] supported on Heim columns [11, 12] and with attached current leads.

Recently a similar approach has been proposed by Sun [13] for testing race track coils for wind power applications as shown in Fig. 7.11.

All direct bolt-on cryocoolers may be designed sleeved or non-sleeved, depending on maintenance requirements. The same can be said for coolers that are used to recondense cryogens, e.g. helium gas. See Figs. 7.12 and 7.13.

There are downsides to both designs. A non-sleeved design requires a good 1st stage pressed contact onto the cooler interface and a work around for any convective parasitic heat loads between 1st and 2nd stage that may arise (in the absence of stratification). One also has to take precautions against air ingress that later could block internal tubing to an immersed magnet making any recondensation impossible. For the sleeved system, a good, repeatable thermal contact at both cryocooler stages is required.

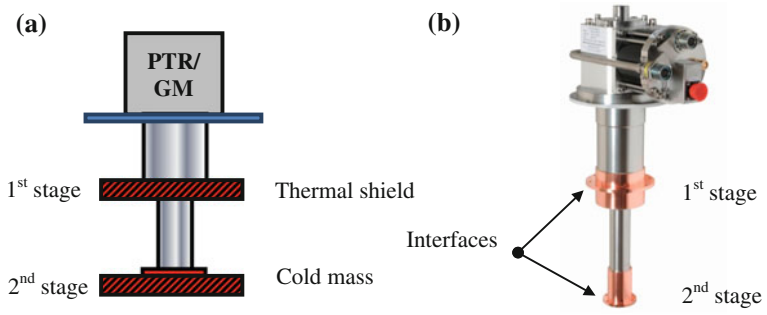

Fig. 7.8 **a** Cryocooler bolted onto thermal shield and thermal mass, **b** SHI 4 K cryocooler RDK 408 D2 with bolt holes at first and second stages (*courtesy* of SHI cryogenics)

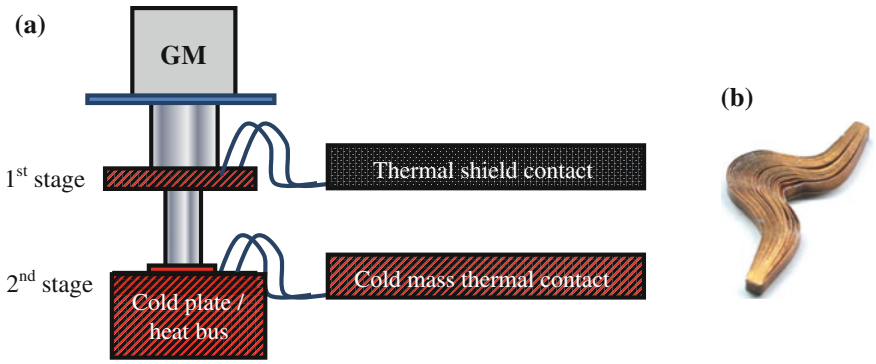

Fig. 7.9 **a** GM or PTR type cryocooler bolted onto cold plate with highly conductive copper or aluminum braids to cold mass (GM type), see also (*1*) in Fig. 7.14. **b** Example of a foil welded copper link

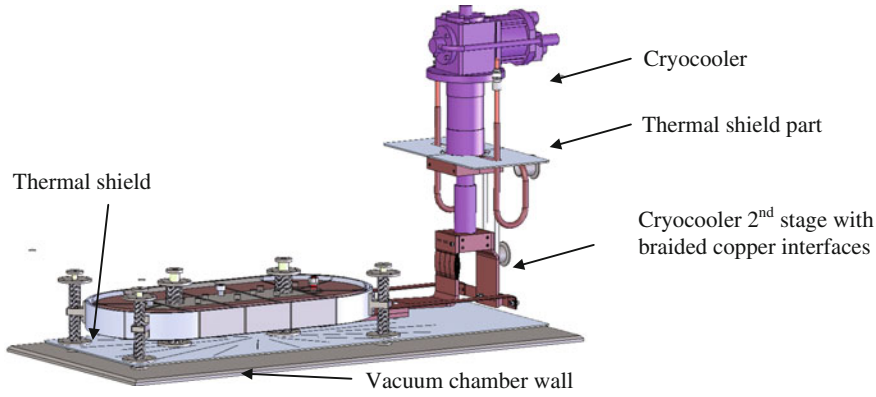

Fig. 7.10 Bolt-on design (vacuum chamber open for clarity), directly to cold plate and race track cold mass with lead in/out

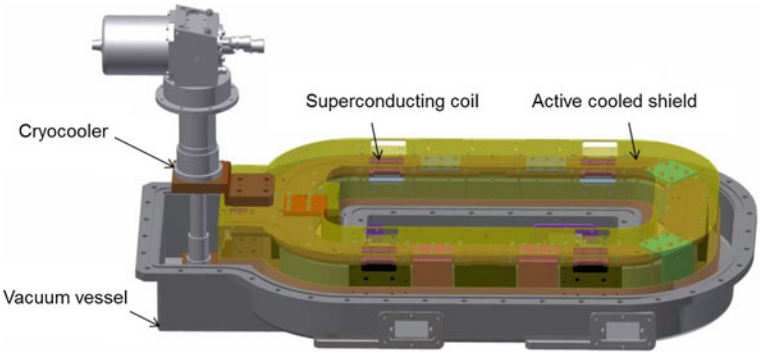

Fig. 7.11 Race-track coil for wind power applications (test bed)

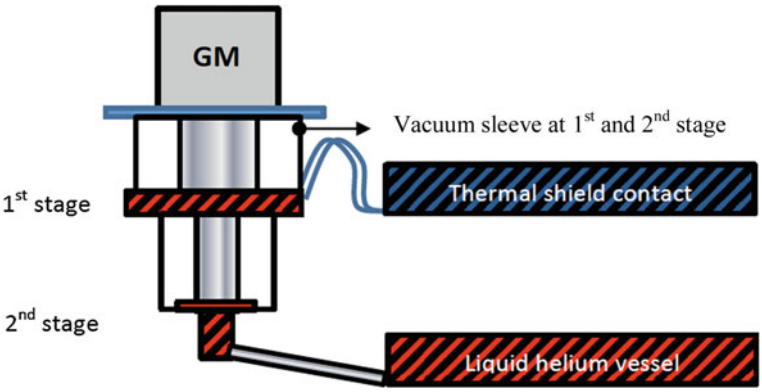

Fig. 7.12 Sleeved cryocooler and with thermal shield contact with liquefaction cup fitted to the second stage

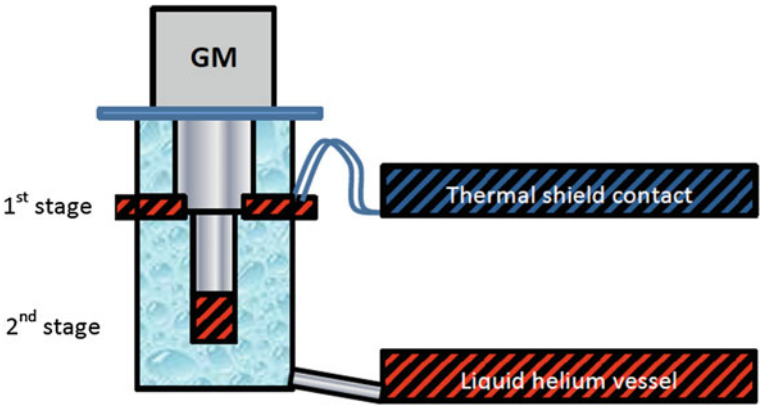

Fig. 7.13 Sleeveless cryocooler, in direct contact with helium gas and link to thermal shield

Preferred contact means across the interface are either Indium or the less costly Apiezon N® grease.

A cooler can also be integrated and made detachable from its contact stages for a number of reasons. For example, in case of a sudden, unplanned power outage and following compressor shut down resulting in a loss of cooling power, a thermal short would be created that leads to high heat loads to the cooling components (e.g. thermal shield, current leads, cold mass). For large thermal mass cooling (e.g. during cool down) a shielded drive mechanism can be installed. The drive mechanism moves the cooler cold end to the cold mass interface maintaining a specified contact pressure that compensates for the cold mass shrinkage. To avoid a permanent parasitic heat load on the cold mass that can be substantial for larger coolers, the cooler is then retracted automatically [14].

Figure 7.14 shows MRI applications using high temperature superconductors and cooling approaches as discussed in this section.

The cryocooler for the so-called open C-magnet is rigidly and sleeveless bolted onto a cold plate. From the cold plate, braids are routed to the copper sheets that are sandwiched between the individual pancake coils. (2) and (3) show various

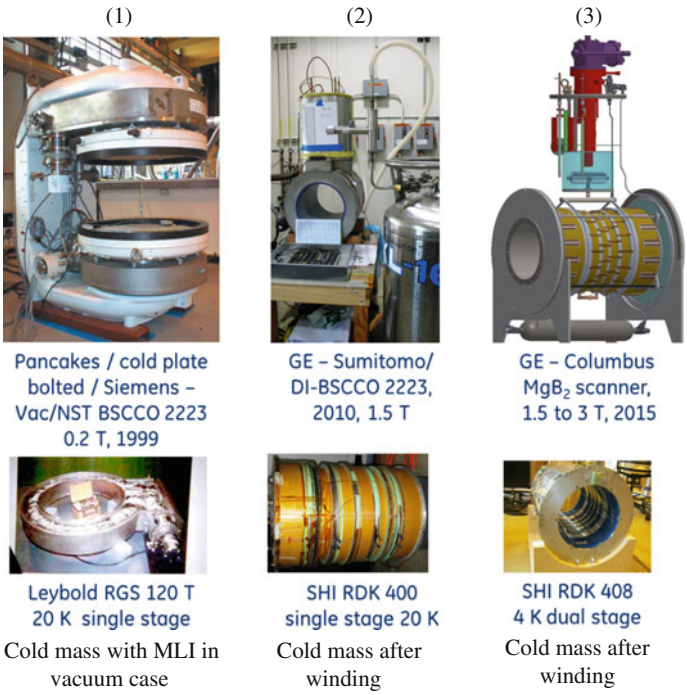

Fig. 7.14 Cryocooler integration methods for small-scale HTS MRI. *1* Cooling technique: conduction cooling cryogen: n/a cooler: single-stage GM [15]. *2* Cooling technique: thermosiphon cryogen: neon, cooler: single-stage GM [16, 17]. *3* Cooling technique: Thermosiphon, dual cryogens: helium or hydrogen, cooler: dual-stage GM [18]

solutions for extremity scanners for different superconducting wires using thermosiphon technology and cryogen liquefaction with zero boil-off.

7.2.4 *Cryocooler Integration Techniques for Special Applications*

Heat pipes can be heat-sunk to a first stage of a cryocooler, preferably for sleeved versions. The cold end of the heat pipe extends to the component that needs to be cooled. Heat pipes generally require no maintenance and, depending on the application, are closed system components that give the opportunity of deeply embedding them in a cryogenic structure.

A further common practice is to heat sink the resistive parts of a current lead or the warm end of a HTS lead to a cryocooler. One little complication here is that one needs to work around the conundrum of requiring good thermal contact and electrical isolation that normally exclude each other.

Last but not least several novel applications have surfaced recently [19]. Cryozone for example attaches a heat exchanger onto the cold stage of a cryocooler, mainly for steady state forced-flow HTS application cooling, e.g. superconducting cables etc. [20] (see Fig. 7.15).

It is also possible to run actively cooled circulation loops with hybrid pulse tube refrigerators combined with circulators and cold flow rectifiers as demonstrated by Feller, Salerno, Nellis et al. [21].

Thus, cryocoolers are playing a key role whenever distributed cooling of large surfaces is required. Gas or liquid circulation through cooling loops is possible using micro pumps, blowers or impellers. For HTS applications, the compressed gas can exit, return to the cooler and become part of the distributed cooling circuit.

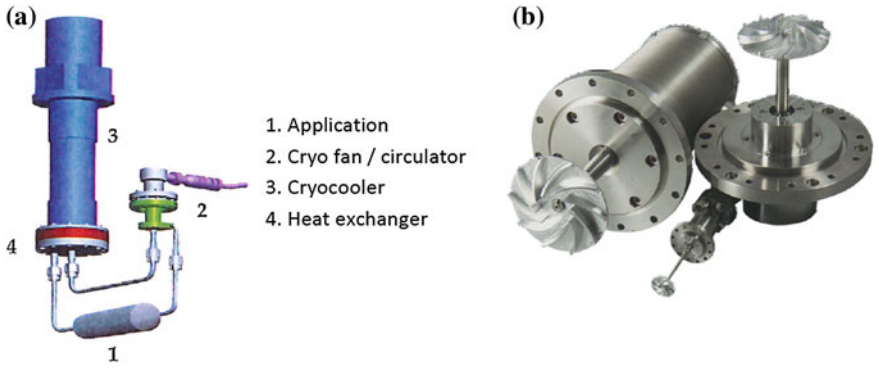

Fig. 7.15 **a** Cryocooler with attached heat exchanger enabling cryogen flow circulation and **b** cryofans (*courtesy* of Cryozone)

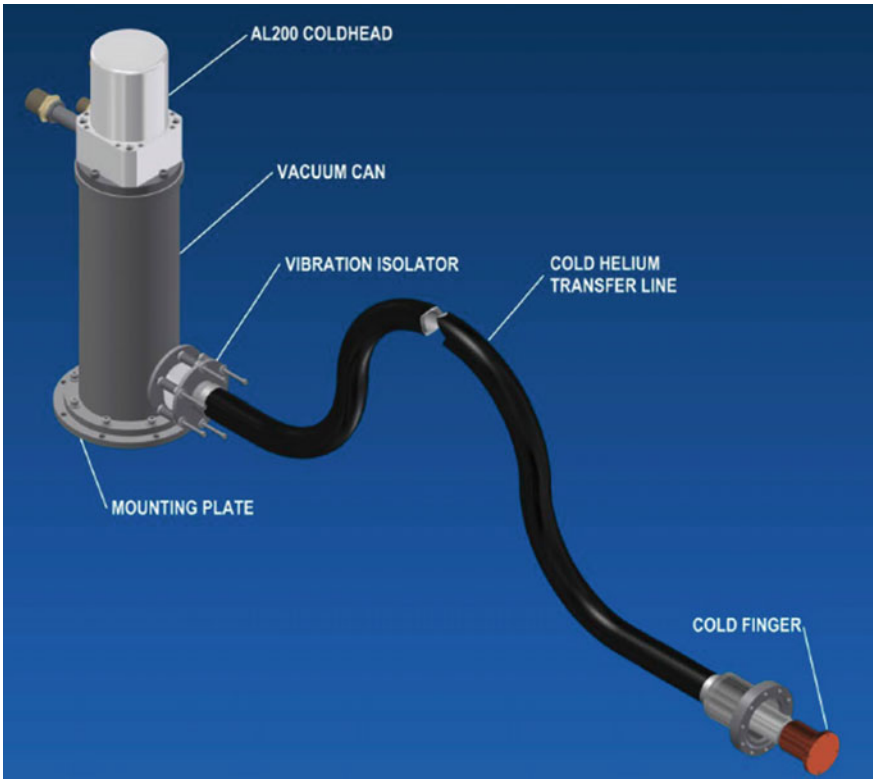

Fig. 7.16 Cryocooler cold finger cooling with cold helium transfer line (*courtesy* of ICC Press)

Some designs for specific applications require operating the cryocooler at a distance from the object to be cooled. One reason could be the better serviceability for the cooler or if vibration transmission to the object should be minimized which otherwise would interfere with a measurement. This kind of "elongation of the cryocooler cold stage" has recently made possible with a novel approach taken by Cryomech [22] shown in Fig. 7.16. This "cold finger" solution delivers very efficient remote cooling of electronic and other components.

7.3 Designing with Inclined Tubes in Cryogenic Systems

When designing cryostats, the engineer occasionally may be tempted to introduce tubing, penetrations or gas filled sleeves in an angled orientation. There are a number of reasons for implementing those, either for getting better accessibility to the internal cryostat structure from the top, when patient room height limitations need to be considered or simply for better liquid draining.

In other designs where the cryostat envelope space is tight, gas filled tubes and/or operating under high pressure can only be fitted inclined. Furthermore, cryocoolers themselves are gas filled tubes under pressure, in particular the pulse tube cooler, with its absence of any solid moving piston. The moving piston here is the oscillating gas column itself. Not surprisingly there are operational limits due to inclination for this cooler, as we will see.

So why should the cryogenic designer be careful when routing inclined tubes or a network of pipes? Inclined tubes generally introduce a parasitic heat flow driven by the density difference in the working medium due to the difference in the length of the wall conduction heat path and the resulting heat load that sets up fluid motion within these tubes. If there is only a small deviation required from the vertical it is almost always better to keep the tubing vertical. The answer really depends on how critical it is to maintain the cryostat heat balance and whether any cost increase that may result is acceptable.

Inclined tubes can be classified as follows:

- Inclined tubes (neck tubes/turrets) at low or high operating pressure (open[1]/closed)
- Inclined tubes with pulsating flow at high/low frequency
- Inclined tubes for thermal mass cool-down
- Inclined heat pipes
- Inclined thermosiphons

When designing cryostats we often notice that the heat balance deviates from expected, calculated values. It is then we look out for parasitic heat loads that may have been missed in the design or at last minute changes in the assembly. As Scurlock noted in 1977 [23], “the boil-off is always 50–100 % greater than the design figures”. This prompted Islam and Scurlock to conduct vapor column flow visualization experiments for vertical and inclined tubes. The team was the first to show in which way the gas column flow changes when tubes are tilted. Tests were performed on wide open tubes as well as on ones with small diameters that are open to atmosphere. It was possible to differentiate between 6 distinct regions in which the flow changes within the column.

Figure 7.17 shows a typical tubing that gives easy access to a liquid reservoir, e.g. for current lead insertion or for filling the reservoir or for using it as a boil-off tube.

This tilt angle was identified as a source of heat leak into the cryogenic liquid storage vessel. Further research detail is given in [24–28]. With the starting interest in pulse tube cooler technology researchers quickly noticed the orientation dependency of the tubing. A typical curve is shown by Kasturirengan [29], (see Fig. 7.18a) for a pulse tube cooler running at 15 bar at a frequency of 1.6 Hz. The inclination angle is shown in Fig. 7.18b. Figure 7.18a shows the convective, or

[1]Open under high pressure in this case means the open end of the tube is connected to a larger gas reservoir under high pressure.

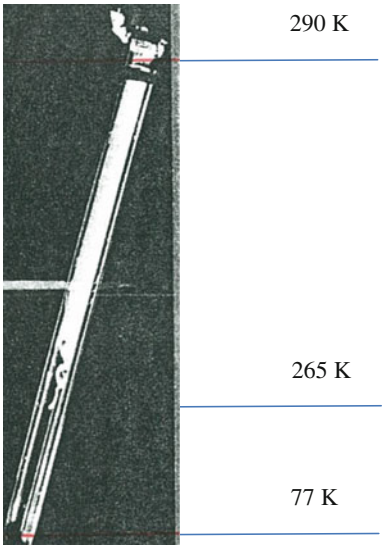

Fig. 7.17 Tilted, open access tube for a cryostat [23]

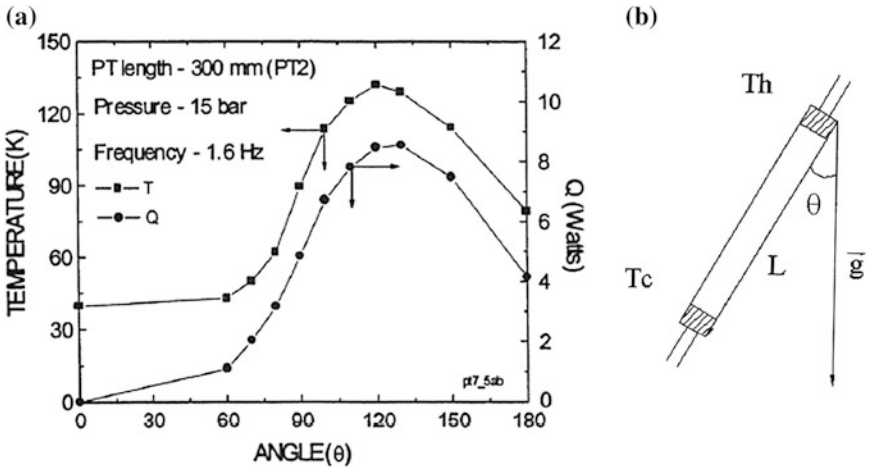

Fig. 7.18 **a** Typical PTR cooling power loss, **b** at different inclination angles [29]

parasitic heat loss that reduces the cooling power at different inclination angles. For high frequency operation this effect is reduced as Thummes reports [30].

The recent research of Langebach and Haberstroh [31] and others is of great value when inserting tubes in cryostats that work under high pressure and are closed or open (closed with reservoirs) at the ends. Why is that important for cryostat designs? Cryostats sometimes are not only used as storage container or for experiments but for housing a cold mass and in particular a superconducting

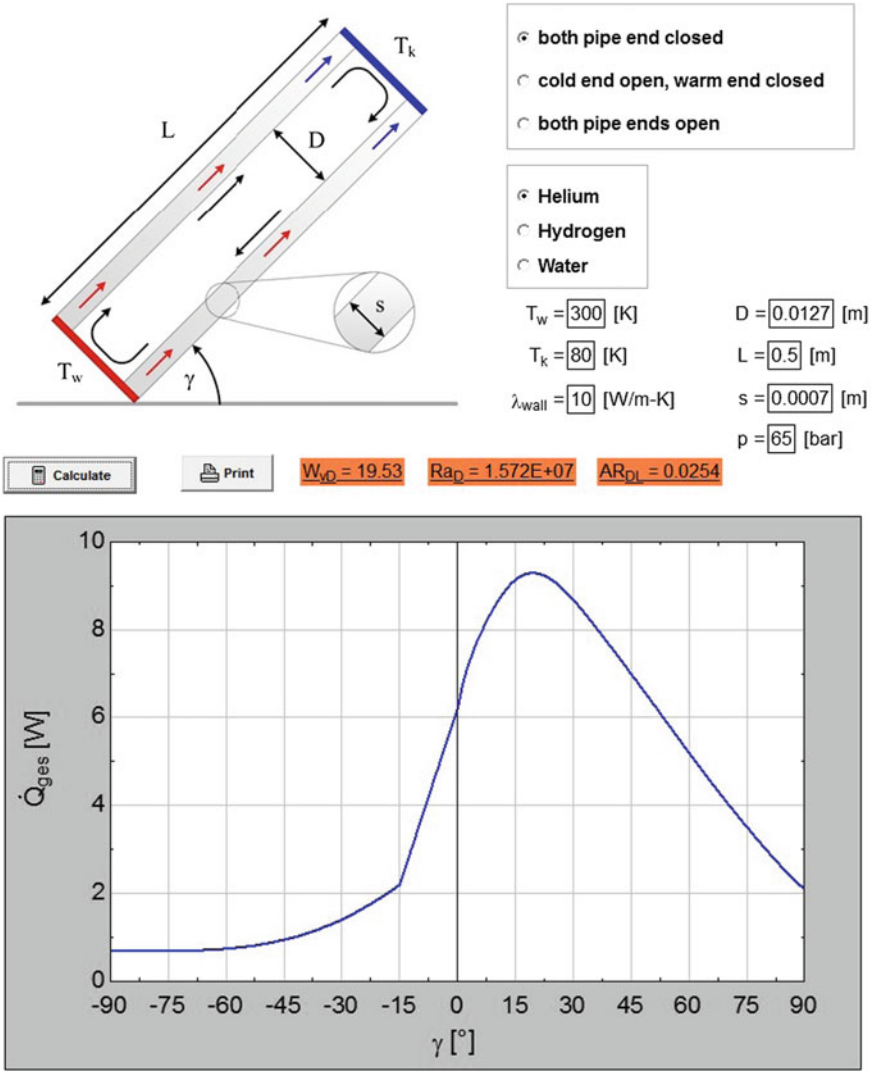

Fig. 7.19 Tilted pipe under pressure—convective behavior (*courtesy* of Langebach)

magnet. The cool-down of a cold mass is often facilitated and accelerated using a heat pipe, a typical, early configuration is given by Begulilowa [32]. In cryogenic designs, very rarely has one the comfort of routing the heat pipe vertically and they most likely will always be inclined. For those instances the computer program developed by Langebach [33] (based on his experimental correlations) calculates the performance loss due to the inclination effect before the heat pipe starts to liquefy at the cold end that is, e.g. during cool-down from room temperature to its operating temperature. Once liquid is formed within the tube and the pressure

within the tube is reduced to its designed operating pressure other curves apply that show the degradation in performance of an unwicked heat pipe at tilted angles.

Referring to Fig. 7.19 −90° defines the tube with its warm end up (T_w) whereas +90° means the cold end is up (T_k). Input parameters are operating pressure in bar, temperature and average thermal conductivity of the tube wall, length, diameter and thickness. Further information is required on whether the tube is closed at both ends or only at one end and what cryogen is used (helium, hydrogen, nitrogen). In his thesis Langebach examines different tubes at different boundary conditions and Raleigh numbers and gives a range of methods to prevent convection in inclined tubes from happening. With one of his solutions—the "snake" tube—parasitic heat loads were considerably reduced.

As for the particular use of an inclined thermosiphon tubing, this highlights an interesting aspect that needs further investigation. For some applications, boundary conditions and operating conditions it may be beneficial to incline a thermosiphon tube whenever a high quality thermal short is required, e.g. during an initial cool-down.

7.3.1 Pitfalls

A horizontal thermosiphon tubing or a horizontal manifold is known not to work and should be avoided as it stops the bubble movement (gas bubble entrapment) and causes flow instabilities. For bubbles to move towards a recondensing surface, a horizontal inclination angle of at least 5° is required.

7.4 Cryogenics for Cryostats: Pressure Rise

All cryostats, such as those used for accelerator magnets, SC generators or large scale storage vessels require design against overpressure. In the event of a superconducting magnet "going normal" or by a preceding rupture of the vacuum vessel, the stored magnet energy of several MJ is quickly dissipated to the helium bath as well as to the magnet former itself (Fig. 7.20).

The amount of heat transferred to the bath is a function of the magnet energy content, the current decay time constant, the transient heat transfer to liquid helium (the obtainable heat flux density (see Table 7.3) in W/cm^2), vessel volume and fill level, the set pressure for the relief valve or burst disk, the magnet former surface structure, as well as type and orientation of the latter. Each liter of liquid helium at 4 K creates 700 L of gaseous helium that need to be discharged safely; for a 3 T magnet cryomodule this would amount to 1.4 million gas liters. External quench gas capture is therefore difficult. Using a cryocooler for reclaiming the quench gas and associated cooldown usually is not feasible within a reasonable timeframe for standard bath-cooled cryomodules. If possible, transfer liquid helium back into

Fig. 7.20 Quench gas release through quench duct after decommissioning a cryomodule for MRI (MRI magnet installed in hospital basement)

Table 7.3 Typical heat flux densities in W/cm^2 for cryostats (collapse and/or quench) [34]

Designs—typical configuration	Flux
Superinsulated bath cryostat	0.6
Liquid helium transport can with gas-cooled shields	2.0
Helium vessel without insulation	3.8
Usually for quench calculations	4–5

dewars rather releasing helium to outer space when decommissioning complete cryomodule systems.

7.4.1 Quench Pressure Rise in Cryostats and Quench Duct Sizing—A Modeling Example

Predicting quench pressure rises in cryomodules is generally a difficult task, but nevertheless necessary. The possible increase in 4 K magnet temperature to 40–50 K after a quench—depends on the chosen coil structure, the coil former material and mass as well as on the amount and type of wire and coil configuration (e.g. race track coil or solenoid). When designing the cryostat the important operating conditions have to be fulfilled, with the magnet quench posing all greatest challenge. Peak mass flow rates of up to 5 kg/s leaving the cryostat at a temperature of 10 K, partly accompanied by liquid helium expelled at the turret exit (see position 2 in Fig. 7.21) are not unheard of.

Quench pressure rise modeling has been attempted previously with forced flow fusion type magnets [35, 36], accelerator quadrupole magnets [37] and smaller solenoids [38], but only very little so far has been done on many magnet systems, see for example in [39]. An excellent attempt in how to solve the similar cryostat

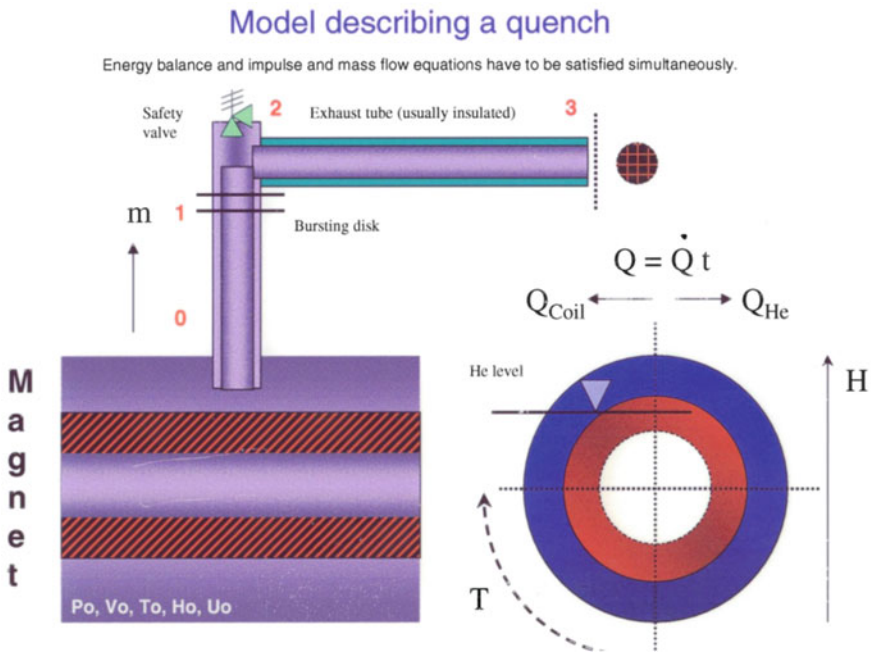

Fig. 7.21 Basic quench parameters for state-of-the-art cryostats and energy transfer

vacuum collapse problem has been pointed out by the late Walker [40] on a 19,000 L helium storage tank at Fermi lab.

For a magnet system, pressure P, volume V, temperature T, enthalpy H and internal energy I at the initial state 0 are given. Once the magnet dissipates its energy to coil former and helium bath, the pressure rise can be described as isochoric, followed by an isentropic expansion [41] through the valve system (Fig. 7.21: position 2) once the valve opens, and for reasons of simplicity the flow can be regarded as adiabatic through the quench duct. The stepwise iterative calculation with real gas properties is rather complex involving compressible friction flow close to the speed of sound simultaneously satisfying gas dynamic equations for Helium (Fanno line) with the associated transient heat transfer. Figure 7.22b shows a theoretical quench pressure calculation result. Green line (bar) = quench pressure decay (dip after burst disk opens), black (kg/s) = volume flow out of cryostat, red (K) = temperature rise of the helium vessel over 6 s. Safe discharging of quench gas requires careful design of the turret diameter and providing and maintaining an unblocked gas passage. The gas transfer mechanism from the cryostat to ambient atmosphere requires a reliable safety valve, a burst disk and a quench gas line of sufficient diameter, the latter depending on the customer siting requirements. Figure 7.22a shows typical quench rates in state-of-the-art high-energy magnets in cryomodules. Note the sudden rise in pressure from 0 to 5 psi within 2 s. The entire duration of the gas release depends mainly on the

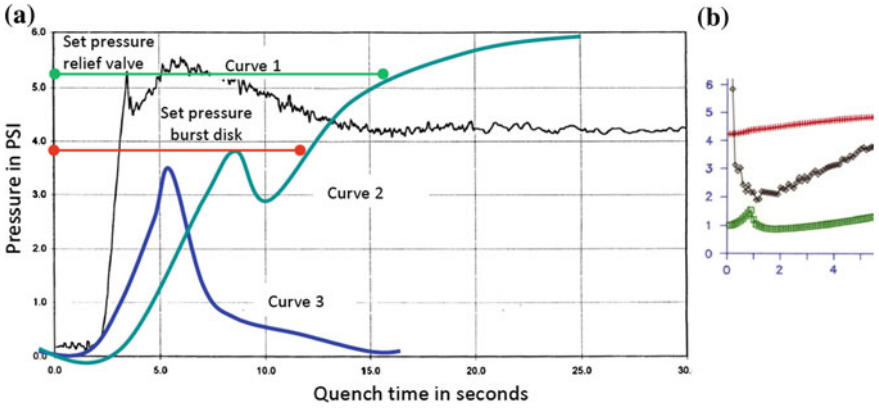

Fig. 7.22 **a** Typical examples of quench test results for cryo-modules cryostats, **b** modeling

opening diameter of the quench turret and on the discharging rate of the cryostat valve. In the example in Fig. 7.22a, curve 1, the total magnet quench time is approx. 5 s; after that time, the pressure and mass flow starts to decay exponentially.

Curve 1 represents the course of the quench pressure when selecting a relief valve that could cause potential problems for several reasons: although the quench valve opens and the pressure drops immediately, the quench pressure still rises again 5 s after the relief valve opens and remains constant. Three problems are highlighted with this example. Firstly, should the gas flow see a further restriction, e.g. due to ice formation, the pressure increase could make the burst disk blow which is undesirable since then the magnet is exposed to ingress of air and further turret ice-up. Secondly, in case the flow restriction in the safety valve increases even further and, if the burst disk is chosen with a too small a diameter the quench pressure itself can exceed the design pressure of the cryostat and invalidate the coding requirements for this cryostat vessel. Lastly, the long quench duration itself leads to icing up of further vent line components and faults. Design guidelines are given in [42, 43]. Curves 2 and 3 show the course of the quench pressure curve for a burst disk opening pressure of 4 psi (red line). Curve 3 safely releases the helium gas with sufficient discharge rate and a high enough kV-value, whereas curve 2 compromises the pressure vessel design by considerably exceeding the design pressure with the danger of rupturing the helium vessel or fitted components. It is also interesting to note that the opening diameter initially helps to quickly release gas into the quench duct, hence the dip in pressure. There is however a sharp increase one needs to watch out for when fitting long quench ducts. Curve 2 is also a typical example where the quench duct is too long leading to a back pressure in the cryostat. In this case the diameter has to be increased or the number of pipe bends reduced.

7.5 Advanced Cryostat Cryogenics—Carbon Footprint Considerations

"Advanced cryogenics" [44] aims to reduce the liquid helium inventory by introducing heat pipe technology, creating a basically "near-dry" type, conduction-cooled magnet as introduced by the accelerator magnet industry in the 1970s. One of the downsides of a reduced cryogenic volume is the longer time needed to recool the magnet back to operating temperature. On a more positive note any loss of vacuum in the cryostat triggering a quench for example, no longer requires satisfying the high safety ordinance efforts as required for a 3000 L helium vessel.

References

1. W. Stautner, Quantitative energy balance analysis in cryostats, in *Physicist's Conference*, *Oral presentation*, Münster, 1984
2. G. M. Dusinberre, *Heat Transfer Calculation by Finite Differences* (International Text book Company, 1960)
3. G.M. Dusinberre, *Numerical analysis of heat flow* (McGraw Hill, 1949)
4. D. Croft, D. Lilley, *Heat Transfer Calculations Using Finite Difference Equations* (Applied Science Publishers, 1977)
5. P. Hanzelka, I. Vejchoda, Academy of sciences of the Czech Republic, Institute of Scientific Instruments (2003)
6. G. Arahonian, L.G. Hyman, L. Roberts, Behavior of power leads for superconducting magnets. Cryogenics **21**, 145 (1981)
7. J.M. van Oort, E.T. Laskaris, P.S. Thompson, B. Dorri, K.G. Herd, A cryogen-free 0.5 Tesla MRI magnet for head imaging. Adv. Cryog. Eng. **43**, 139–147 (1998)
8. K.G. Herd, E.T. Laskaris, P.S. Thompson, A dual refrigerator assembly for cryogen-free superconducting magnet applications. IEEE Trans. Appl. Supercond. **5**, 185–188 (1995)
9. J R. Ross, M. Donabedian, Spacecraft thermal control handbook. Cryogenics **II** (2003)
10. W. Stautner, K. Sivasubramaniam, E.T. Laskaris, S. Mine, J. Rochford, E. Budesheim, K. Amm, A cryo-free 10 T high-field magnet system for a novel superconducting application. IEEE Trans. Appl. Supercond. **21**, 2225–2228 (2011)
11. J.R. Heim, The heim column, National accelerator laboratory, report TM.334A (1971), pp. 1–21
12. G. Hartwig, Support elements with extremely negative thermal expansion. Cryogenics **35**, 717–718 (1995)
13. J. Sun, S. Sanz, H. Neumann, Conceptual design and thermal analysis of a modular cryostat for one single coil of a 10 MW offshore superconducting wind turbine, in *IOP Conference Series*, vol. 101 (2015) p. 012088
14. W. Stautner, Remote actuated cryocooler for SC generator and method of assembly the same, US20140100113A1
15. F.J. Davies, W. Stautner, A.F. Byrne, M. Wilson *An HTS magnet for whole-body MRI*, EUCAS'99
16. W. Stautner, K. Amm, E.T. Laskaris, M. Xu, X. Huang, A new cooling technology for the cooling of HTS magnets. IEEE Trans. Appl. Supercond. **17**, 2200–2203 (2007)

17. W. Stautner, M. Xu, E.T. Laskaris, G. Conte, P.S. Thompson, C. van Epps, K. Amm, The cryogenics of a thermosiphon-cooled HTS MRI magnet—assembly and component testing. IEEE Trans. Appl. Supercond. **21**, 2096–2098 (2011)
18. W. Stautner, M. Xu, S. Mine, K. Amm, Hydrogen cooling options for MgB2-based superconducting systems, in *AIP Conference Proceedings*, vol. 1573 (2014), p. 82
19. W. Stautner. K. Amm, M. Xu, Cooling systems for HTS applications—overview and critical assessment, IWC-HTS plenary talk 1, Matsue-Shi (2015)
20. H. Vermeulen, Cryogenic circulators: the solution for cooling problems? Cold Facts **29**(2), 49–48 (2013)
21. K.R. Feller, L.J. Salerno, A. Kashani, B.P. Helvensteijn, J.R. Maddocks, G.F. Nellis, Y. B. Gianchandani, Technologies for cooling of large distributed loads, AIAAA, 092497 (2008)
22. C. Wang, E. Brown, A. Friebel, A compact cold helium circulation system with GM cryocooler, in *18th International cryocooler conference ICC*, Syracuse (2014)
23. M.S. Islam, R.G. Scurlock, Qualitative details of the complex flow in cryogenic vapor columns. Cryogenics 655–680 (1977)
24. P. Lnyam, A.M. Mustafa, W. Proctor, R.G. Scurlock, Reduction of the heat flux into liquid helium in wide necked metal dewars. Cryogenics 242–247 (1969)
25. M.S. Islam, R.G. Scurlock, Analysis of solid vapor heat transfer in helium vapor columns at low temperatures. Cryogenics 323–328 (1978)
26. M.S. Islam, D.J. Richards, R.G. Scurlock, The influences of thermal stratification and flow interaction on the enhanced natural convective heat transfer at low temperatures. Cryogenics 319–325 (1978)
27. J. Boarman, P. Lynam, R.G. Scurlock, Complex flow in vapor columns over boiling liquids. Cryogenics 520–523 (1973)
28. P. Lnyam, W. Proctor, R.G. Scurlock, Reduction of the evaporation rate of liquid helium in wide necked dewars, in *Heat Flow Below 100 K*, no. 2 (International Institute of Refrigeration, Paris, France, 1965), pp 351–247
29. S. Kasturirengan, S. Jacob et al., Experimental studies of convection in a single stage pulse tube refrigerator. Adv. Cryog. Eng. **49**, 1474–1481 (2003)
30. G. Thummes et al., Convective heat losses in pulse tube coolers: effect of pulse tube inclination. Cryocoolers **9**, 393–402 (1997)
31. R. Langebach, C. Haberstroh, Natural convection in inclined pipes—a new correlation for heat transfer estimations, in *AIP Conference Proceedings*, vol. **1573** (2014), pp. 1504–1511
32. R. Bewilogua et al., Application of the thermosiphon for precooling apparatus. Cryogenics **6**, 34–36 (1966)
33. R. Langebach, Wärmeeintrag durch geneigte Rohrleitungen in kryogene Speicherbehälter, Dissertation, TUD press, 2013, URL: http://books.google.de/books?id=Cez5nAEACAAJ
34. W. Lehmann, Internal report, Safety aspects LHe cryostats and LHe transport containers, Research Center Karlsruhe, Report 08.01.01P04B (1978)
35. J.R. Miller, ORNL, Pressure rise during the quench of a superconducting magnet using internally cooled conductors (1980), pp. 321–329
36. P.H. Eberhard, et al, Lawrence Berkeley Lab, Quenches in large superconducting magnets, in *Proceedings of 6th international Conference on Magazine Technology (MT 6)*, Paper 75, Bratislava (1977), pp. 654–662
37. K. N. Henrichsen, et al, Analysis of some resistive transitions in the ISR super-conducting quadrupole magnets. Adv. Cryog. Eng. **27**, 245–256 (1982)
38. V. Kadambi, B. Dorri, Current decay and temperatures during superconducting magnet coil quench. Cryogenics 157–164 (1986)
39. B. Seeber, Handbook of applied superconductivity, in *Pressure increase during a quench*, Vol. 2, Figure G2.2.24 (Stautner) (1998), p. 1235
40. R.J. Walker, Calculation of the pressure rise in the Fermilab 19000 l helium dewar, Adv. Cryog. Eng. **29**, 777–784
41. R.J. Walker, private communication (1985)

42. G. Bozóki, *Überdrucksicherungen für Behälter und Rohrleitungen*. Verlag TÜV Rheinland (1977)
43. W. Lehmann, *Sicherheitsauflagen beim Engineering von LHe- und LN2-Apparaten und –Anlagen,* Research Center Karlsruhe, Report 03.05.01P02A (1982)
44. Y. Lvovsky, W. Stautner, Novel technologies and configurations of superconducting magnets for MRI. Supercond. Sci. Technol. **26**(9), article id. 093001 (2013)